Simulation of Proppant Transport in Fractures with DNS-Derived Drag Laws

Xiaoqi Li and Xiaolong Yin
Petroleum Engineering Department
Colorado School of Mines

Hydraulic fracturing and proppant transport

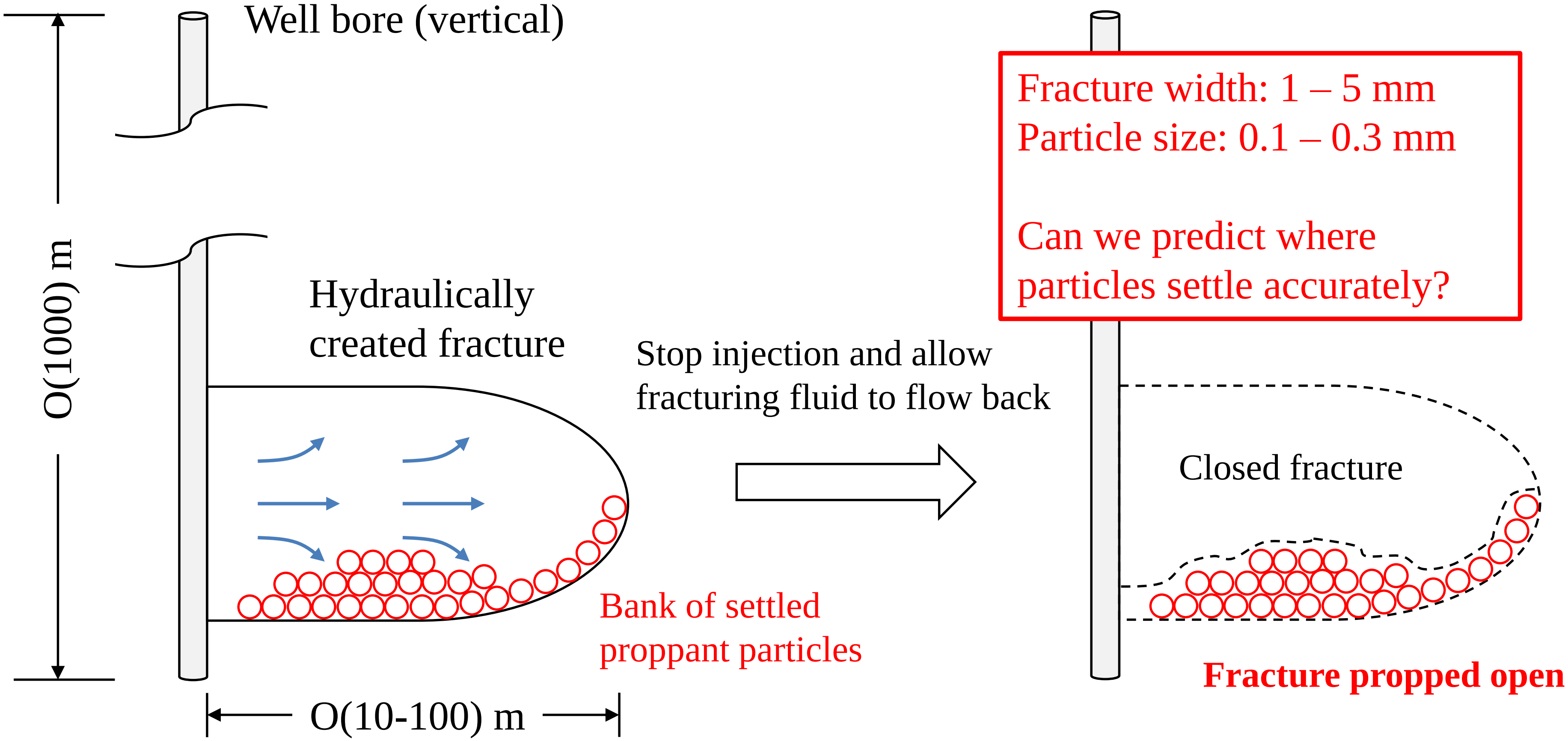

Drag force in Euler-Euler model

- Momentum equation in MFIX two-fluid model

Fluid phase

$$\frac{\partial}{\partial t}\left[(1-\phi)\rho_f \mathbf{u}_f\right] + \nabla\cdot\left[(1-\phi)\rho_f \mathbf{u}_f \mathbf{u}_f\right] = \nabla\cdot\boldsymbol{\sigma}_f + (1-\phi)\rho_f \mathbf{g} - \mathbf{I}_{f\to p}$$

Fluid stress

Fluid-particle interaction

Solid phase

$$\frac{\partial}{\partial t}\left(\phi\rho_p \mathbf{u}_p\right) + \nabla\cdot\left(\phi\rho_p \mathbf{u}_p \mathbf{u}_p\right) = \nabla\cdot\boldsymbol{\sigma}_s + \phi\rho_s \mathbf{g} + \mathbf{I}_{f\to p}$$

Solid stress

Fluid-particle interaction includes generalized buoyancy, **drag**, lift, virtual mass, etc.

Common drag closures for monodisperse particle suspensions

Stokes drag: Single particle, zero Re

$$\mathbf{F}_{f\to p} = 3\pi\mu d\left(\mathbf{u}_f - \mathbf{u}_p\right) \Rightarrow \beta = 18\phi\mu/d^2$$

Schiller-Naumann:
Single particle, finite Re

Wen-Yu drag
Particles setting in groups

Ergun equation
Flow through dense particle assemblies

Gidaspow drag = Wen-Yu (ϕ < 0.2) or Ergun (ϕ > 0.2)

HKL (Hill-Koch-Ladd)

BVK (Beetstra-van der Hoef-Kuipers)

Need for drag closures for proppant transport

- Proppant transport always occurs in **narrow** fractures
- Fractures can be **inclined**
- Settling velocity may be affected by **cross flow**
- Fracturing fluid can be **non-Newtonian**
- Proppants can be **non-spherical**
- Proppants are **polydisperse**
- Fracture surfaces are **rough**

We considered three of the above effects, and derived new drag laws using DNS data

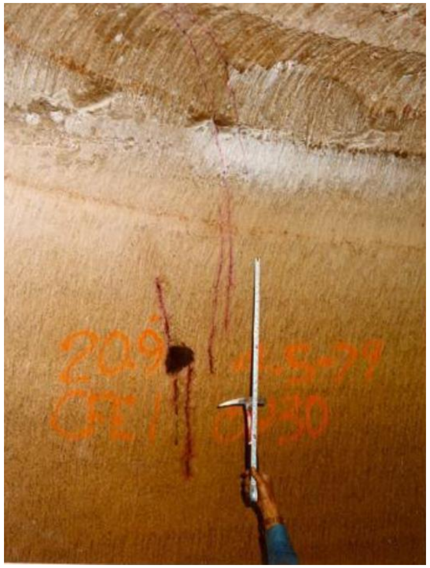

DOE Mineback experiments
N. R. Warpinski et al. (1981)

Setup of LB DNS

- Vertical fractures

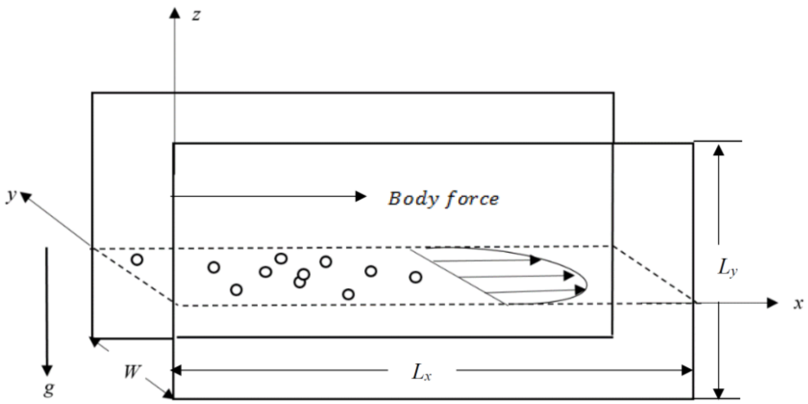

x, *z*: periodic boundaries
y: solid wall
g: along *z*
x: direction of cross flow
L_x/d and L_z/d: about 10
Particle is resolved by 10 LB grid

- Inclined fractures

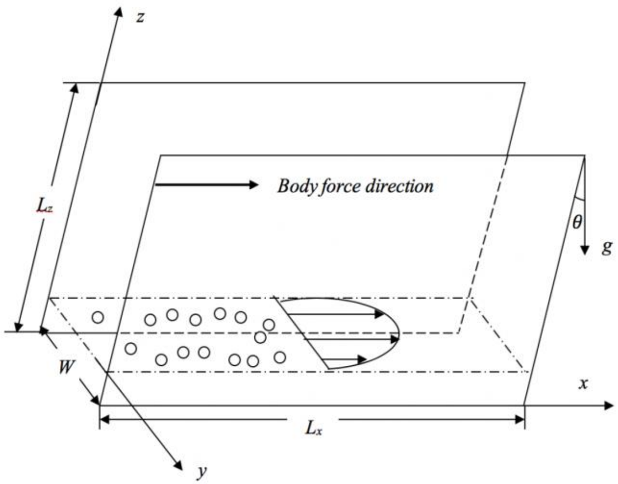

Same as left (vertical) except that
g: has an angle to the z

Dimensionless groups

Archimedes number	$\mathrm{Ar} = \dfrac{gd^3\rho_f\left(\rho_p - \rho_f\right)}{\mu^2}$	20, 71, 319	
Density ratio	$\rho^* = \dfrac{\rho_p}{\rho_f}$	1.1, 2.0, 2.5	
Gap-to-particle size ratio	$W^* = \dfrac{W}{d}$	1.5, 3.0, 5.0	
Reynolds number of cross flow	$\mathrm{Re}_x = \dfrac{\rho_f \langle u_x \rangle W}{\mu}$	1, 3, 10, 30	
Solid volume fraction	ϕ	0.05 to 0.20	
Inclination angle	θ	0°, 15°, 45°, 75°	

Most these dimensionless numbers are realistic, except Re_x. Real Re_x can be as high as 10^4.

Vertical fractures – results

Clear trends / effects

- Settling velocity increases with increasing W^*
- Settling velocity increases with increasing Ar
- Settling velocity decreases with increasing ϕ

Re_z: Settling Reynolds number
Open symbol: $\phi = 0.05$
Filled symbol: $\phi = 0.10$
$\rho^* = 1.1$, $Re_x = 1.0$

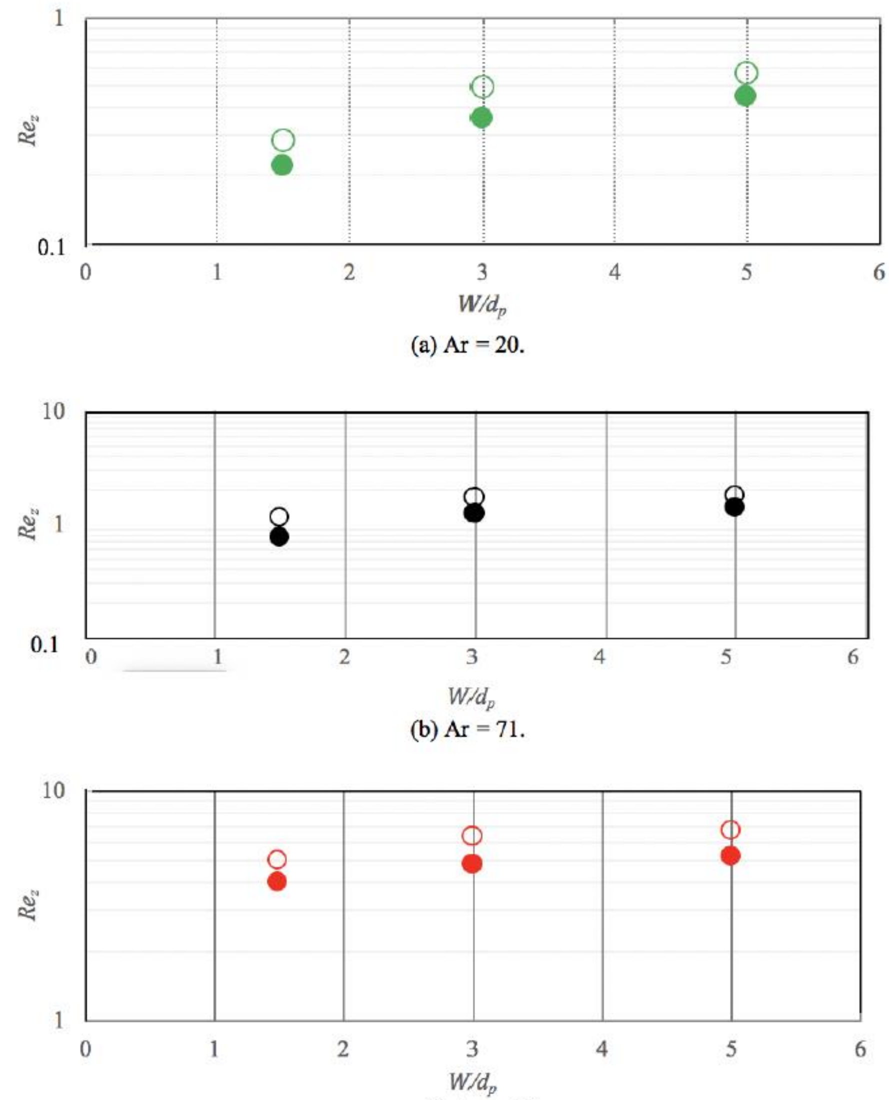

(a) Ar = 20.
(b) Ar = 71.
(c) Ar = 319.

Vertical fractures – results

No clear trends

- Settling velocity is nearly independent of Re_x **in the range (1, 30)**

Re_z: Settling Reynolds number
Various symbols: different Re_x
$\rho^* = 1.1, \phi = 0.05$

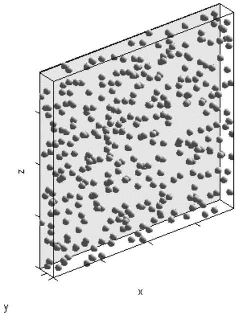

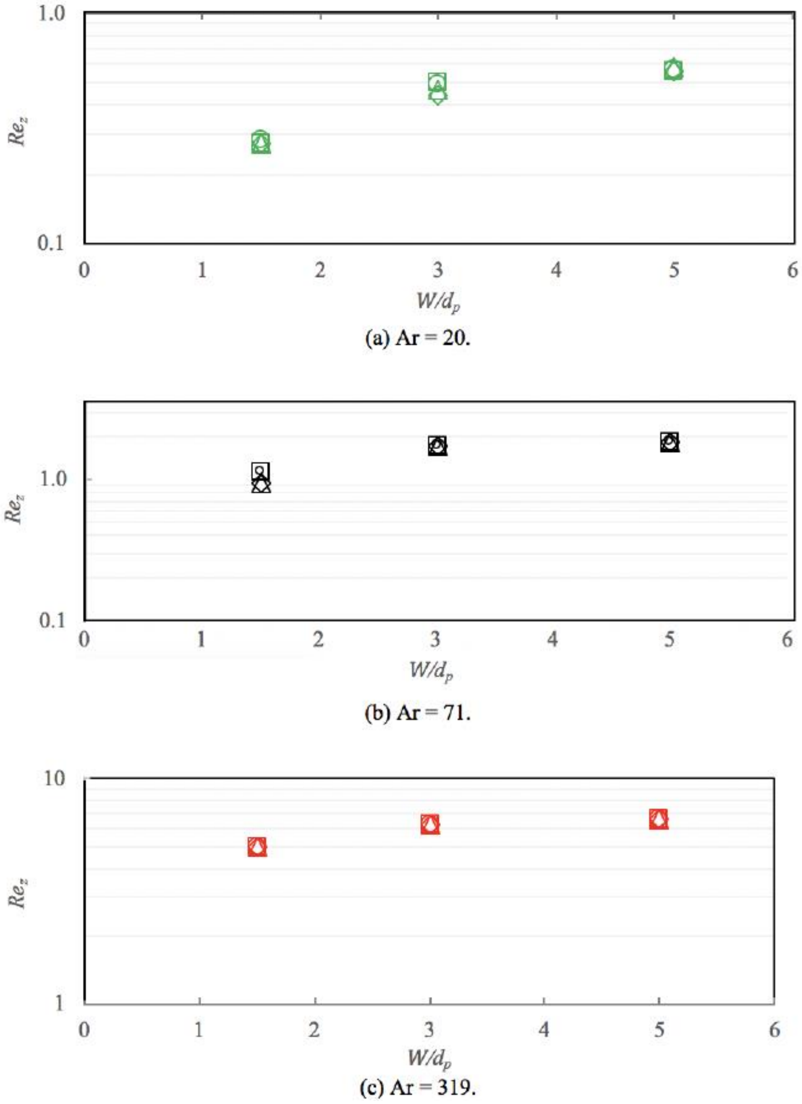

Vertical fractures – results

No clear trends

- Settling velocity is nearly independent of ρ^* **once Ar is fixed**

Re_z: Settling Reynolds number
Various symbols: different ρ^*
$\phi = 0.05$, $Re_x = 1.0$

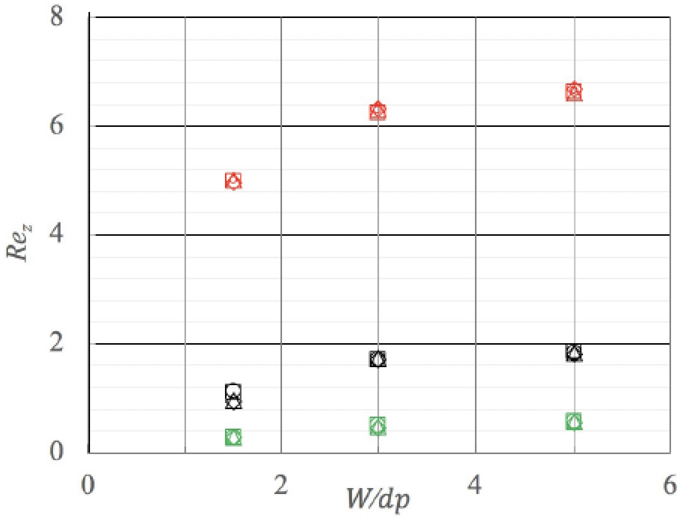

Green: Ar = 20
Black: Ar = 71
Red: Ar = 319

Vertical fractures – correlation for the settling velocity

At this time, we are using a quadratic correlation to fit & present the data

Proppant / fluid properties

Settling velocity of particles in a slurry

Settling velocity of particles between walls

g, d, μ → (Schiller-Naumann) → Re_0 → (Richardson-Zaki) → Re_{RZ} → Re_z

Richardson-Zaki

Schiller-Naumann

$$\mathrm{Re}_{RZ}/\mathrm{Re}_0 = (1-\phi)^{n(\mathrm{Re}_0)}$$

Settling velocity of a single particle

$$\frac{\mathrm{Re}_z}{\mathrm{Re}_{RZ}} = \frac{A(\mathrm{Ar},\phi)}{W^{*2}} + \frac{B(\mathrm{Ar},\phi)}{W^{*}} + C(\mathrm{Ar},\phi)$$

MFIX simulations with BVK law and the new drag law

BVK

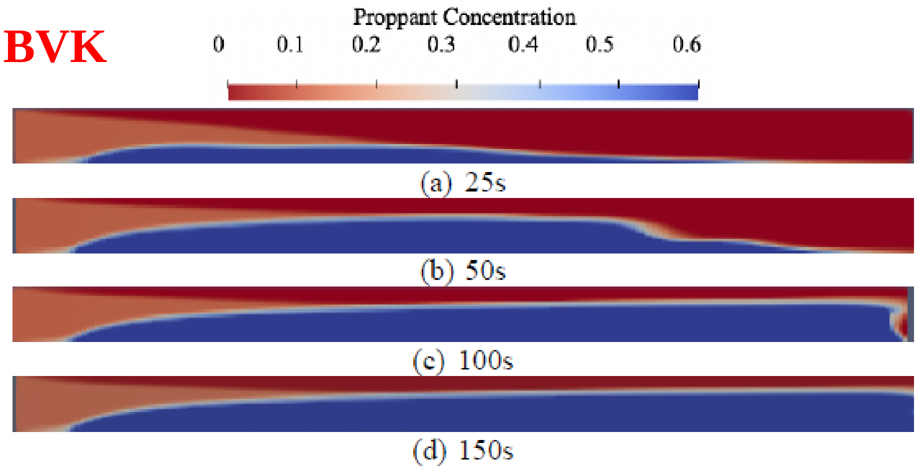

NEW

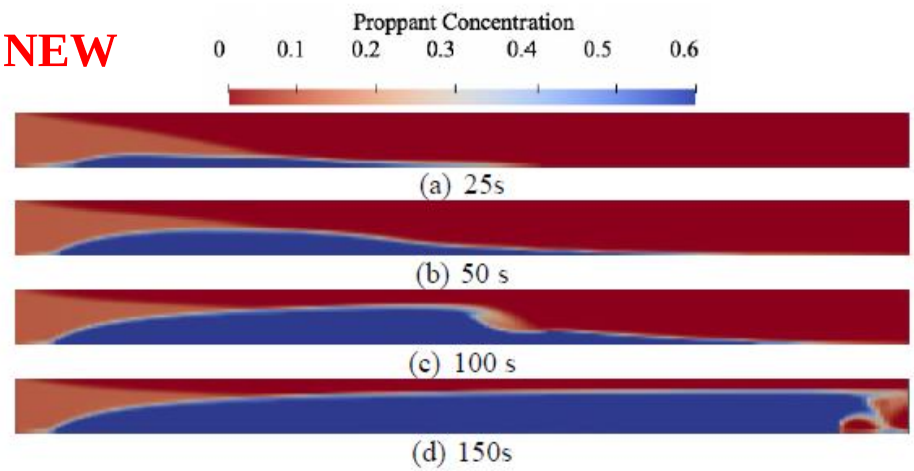

Simulation parameters:

Dimensionality = 2

Domain = 0.1 m × 1 m

d = 0.3 mm, μ = 1 cp, g = 9.8 m/s^2

W = 1.5 mm, ρ^* = 2.0, ϕ = 0.10

$\langle u_x \rangle$ = 0.5 m/s

In the new drag law, proppant bank develops less rapidly primarily because the effect of walls. In terms of height, the new drag law predicts a slightly taller proppant bank

Verification – experiment of Patankar et al. (2003)

Patankar et al., 2003. *Int J Multiph Flow* 29: 475–494.

- Experimental parameters
  - L_x = 244 cm, L_z = 30.4 cm, W = 8 mm
  - Proppant 20/40 Ottawa sand (0.6 mm), ρ = 2650 kg/m^3
  - Fluid viscosity = 1 cp
  - Slurry rate = 284 cm^3/s, proppant volumetric rate = 40 cm^3/s
- Dimensionless numbers
  - Ar = **3496**, Re_x = **960**, ρ^* = 2.65, W^* = **13**, ϕ = 0.14
- Results
  - Experimentally measured height of proppant bank = **28.2 cm**
  - MFIX with BVK – **23.3 cm**
  - MFIX with new drag law – **27.3 cm**

Some numbers are clearly outside the range of DNS data

New drag law still generated more accurate prediction

Summary

- Solid walls significantly hinder the settling velocity
- Cross flow (**with moderate Re**) does not seem to affect settling velocity
- Particle-fluid density ratio does not seem to affect settling velocity
- DNS-derived drag law when substituted into MFIX gave better prediction in the height of proppant bank compared to default drag laws